

High-Output Nanogenerator by Rational Unipolar Assembly of Conical Nanowires and Its Application for Driving a Small Liquid Crystal Display

Youfan Hu,[†] Yan Zhang,[†] Chen Xu,[†] Guang Zhu, and Zhong Lin Wang*

School of Material Science and Engineering, Georgia Institute of Technology, Atlanta, Georgia 30332-0245, United States

ABSTRACT We present a simple, cost-effective, robust, and scalable approach for fabricating a nanogenerator that gives an output power strong enough to continuously drive a commercial liquid crystal display. Utilizing the conical shape of the as-grown ZnO nanowires, a nanogenerator is fabricated by simply dispersing them onto a flat polymer film to form a rational “composite” structure. It is suggested that the geometry induced unipolar assembly of the conical nanowires in such a composite structure results in a macroscopic piezoelectric potential across its thickness by introducing a mechanical deformation, which may be responsible for driving the flow of the inductive charges between the top and bottom electrodes. A compressive strain of 0.11% at a straining rate of 3.67% s⁻¹ produces an output voltage up to 2 V (equivalent open circuit voltage of 3.3 V). This is a practical and versatile technology with the potential for powering small size personal electronics.

KEYWORDS Nanogenerator, ZnO, conical nanowire

Scavenging energy in our living environment is a feasible approach for powering micro/nanodevices and mobile electronics due to their small size, lower power consumption, and special working environment. Nanomaterials have shown unique advantages for energy conversion, including solar cells,^{1–7} piezoelectric nanogenerators,^{8–16} thermalelectric cells,^{17–19} etc. The type of energy to be harvested depends on the applications. For mobile, implantable and personal electronics, solar energy may not be the best choice because solar is not available in many cases under which the electronic devices will be utilized. Alternatively, mechanical energy, including vibration, air flow, and human physical motion, is available almost everywhere and at all times, which is called random energy with irregular amplitude and frequencies. Nanogenerator (NG) is a technology that has been developed for harvesting this type of energy using well-aligned nanowire (NW) arrays and sophisticated fabrication procedures,^{8–10,13} which may limit its potential for scale up to meet industrial applications.

In this paper, utilizing the conical shape of the ZnO nanowires, a simple, cost-effective, and scalable nanogenerator is presented for producing high output power that is strong enough to continuously drive a commercial liquid crystal display (LCD). Unipolar assembly of the conical nanowires in such a composite structure may result in a macroscopic piezoelectric potential across its thickness by

introducing a mechanical deformation, which dictates the distribution and flow of inductive charges between the electrodes on the top and bottom surfaces of the structure. This is a practical and versatile technology for powering small size personal electronics.

The basic structure of the NG is two metal films sandwiched composite, which is made of unipolar assembly of conical nanowires infiltrated with PMMA (Figure S1 in the Supporting Information). First, a Cr/Au (50 nm/50 nm) metal layer was deposited on a Kapton film (127 μm in thickness, Dupont 500HN) by electron beam evaporation; on the metal film a layer of PMMA (~2 μm in thickness) was spun coated on. The deviation in flatness of the PMMA film was better than 1 nm as measured by atomic force microscopy imaging. The NWs used in our experiments were grown on a solid substrate via vapor deposition process²⁰ with lengths over 30 μm (Figure S2 in the Supporting Information). The NWs have a conical shape due to the fastest growth along the *c* axis and a much slower growth rate in the basal plane. The conical shape has been proven vitally important for the NG presented here, which is to be elaborated next. Then, the conical nanowires (CNWs) together with the substrate were soaked into ethanol; applying an ultrasonic wave effectively chopped off the CNWs from the substrate, forming a freely suspended CNW solution. By dispersing a droplet of the CNW solution onto the PMMA film, the CNWs were fairly uniformly distributed on the substrate surface with their lateral orientations random (Figure 1a,b). The area density of the CNWs on the substrate was low (1400–1500 nanowires per mm²) to avoid overlapping and aggregations among the CNWs. The spin-coating of a thin PMMA layer

* To whom correspondence should be addressed. zlwang@gatech.edu.

[†] These authors contributed equally to this work.

Received for review: 09/10/2010

Published on Web: 00/00/0000



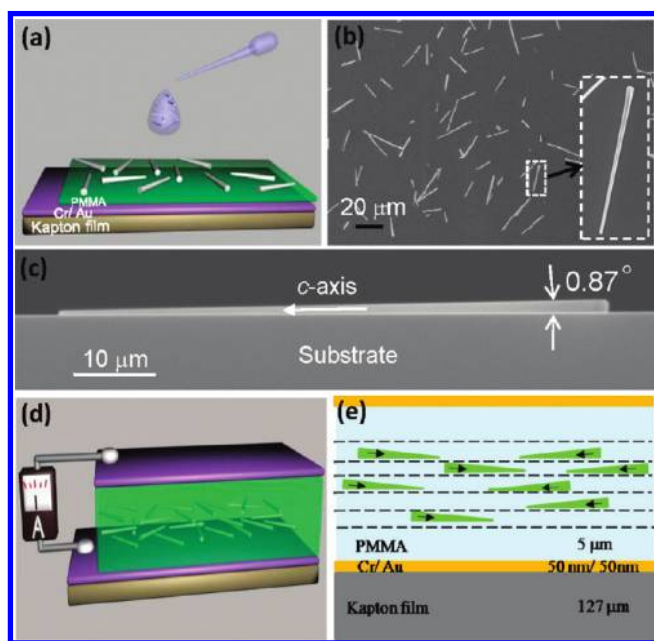


FIGURE 1. Fabrication of the nanogenerator. (a) Schematic diagram showing the fabrication process of the nanogenerator. (b) Scanning electron microscopy (SEM) image showing the CNWs were fairly uniformly distributed on the substrate surface with their lateral orientations random; the insert enlarged image showing the conical shape of the nanowire. (c) Cross-section view SEM image of a conical nanowire laying on a flat substrate. The bottom side surface of the nanowire tightly attached to the substrate, and the conical angle of the nanowire was 0.87° . The white arrowhead indicates that the c axis of the nanowire is pointing downward into the substrate. (d) Schematic image of the fabricated device structure. (e) Schematic diagram showing the idea for the design and the suggested working principle of the structure (see text).

(~ 100 nm) and dropping-on of the ZnO CNW solution were carried out alternately to form a rationally designed “composite” structure. When five cycles of PMMA and ZnO CNWs were deposited alternately, another thicker PMMA layer (~ 2 μm) was deposited, on which a Cr/Au (50 nm/50 nm) metal film was deposited to serve as an electrode (Figure 1d,e). The size of the whole device was about 1.5×2 cm^2 (Figure S1c in the Supporting Information), and it can be robustly bent for many cycles (Figure S1d in the Supporting Information). For electricity generation, the as-fabricated NG was attached to a flexible polystyrene substrate (~ 1 mm in thickness) and an external force strained the assembled structure from the back of the substrate. Therefore, the NG experienced a compressive strain when mechanically agitated; thus the CNWs were under compressive strain as assumed in following calculations.

The working principle of the assembled NG is suggested to be a result of the unipolar assembly of the conical nanowires. The CNWs laid down with random lateral orientation (Figure 1b and Figure S3 in the Supporting Information), while the bottom side surfaces were tightly attached to the flat surface of the substrate (Figure 1c and Figure S4 in the Supporting Information). With considering the [0001] growth direction of the ZnO CNW (Figure S5 in the Support-

ing Information), which represents the polar direction of a NW, the conical shape of the nanowires results in a constructive alignment in their projected polar directions for all of the nanowires in the direction perpendicular to the substrate and pointing downward into the substrate, as shown in Figure 1e, in which the dashed line indicates one cycle of CNWs deposition. The conical shape nanowires and their corresponding c axes are represented by arrowheads, which are the symmetry axes of the nanowires. Owing to the geometrical shape, the component of the c axis of each nanowire in the normal direction of the substrate is $c \sin(\alpha/2)$, where α is the conical angle of the CNW. This projected component of all of the CNWs along the vertical direction constructively adds up, which is the source of piezoelectric polarization across the thickness of the composite structure for creating the piezopotential. The unipolar assembly is probably the key for producing a macroscopic piezoelectric potential in the direction normal to the substrate.

We now calculated the potential generated across the top and bottom electrodes using a simple model as shown in Figure 2a. The entire structure was taken as a free-standing beam with its one end being fixed and a periodical transverse force being applied at its top edge at the end. The voltage drop across the top and bottom electrodes was calculated (see the Supporting Information about the detailed model construction and calculation method). Our model is a capacitor-like plate structure with ZnO CNWs and PMMA as the composited “dielectric” media. With one end of the plate fixed and a transverse mechanical force applied at the other end (Figure 2a), the mechanical deformation of the plate structure was calculated first. Under such a deformation configuration, a distribution of the piezoelectric field in the CNWs was obtained²¹ by assuming a paired CNW model to be discussed next. We purposely placed the CNWs in the region that was under compressive strain to reflect the experimental situation in which the entire NG was under compressive strain with the consideration of backside substrate utilized for the measurements. Lastly, the distribution of the inductive charges in the electrode plates at the top and bottom surfaces were calculated with considering the proper boundary conditions, from which the electric potential difference between the two plates was obtained. Our calculation ignored the coupling between the piezoelectric field and the inductive charges in the electric plates under the first-order approximation. The ZnO CNWs were assumed to be intrinsic without doping. To correctly represent the random distribution of the CNWs on the PMMA film surface, two CNWs with opposite c axes were chosen for the simulation (see details in the Supporting Information), as shown in the model in Figure 2b. The establishment of the induced electric potential difference across the two plate electrodes is the driving force for the flow of electrons in the external load. Although the magnitude of the potential difference depends slightly on the relative depth of the CNWs in the NG due to variation in local strain, the physical picture

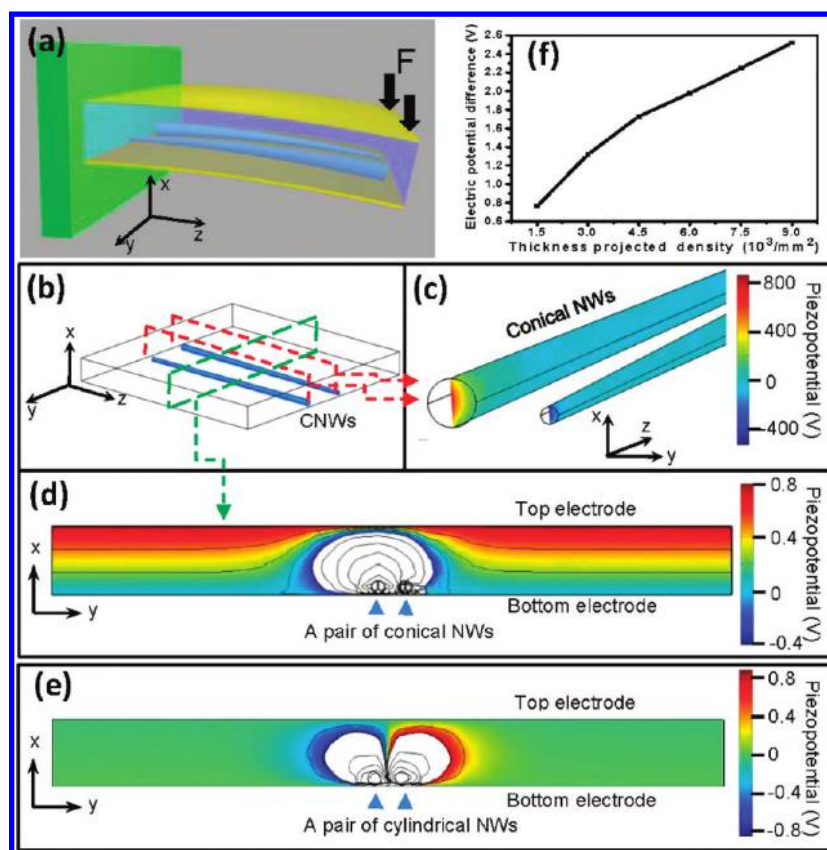


FIGURE 2. Simulation of the nanogenerator. (a) Schematic model showing the setup for measuring the energy conversion. The polystyrene substrate used to hold the NG at its upper side, where the force F is applied, is not shown here for clarity of presentation. The CNWs are under compressive strain during the deformation. (b) The unit cell and model used for calculating the potential distribution across the top and bottom electrodes of the NG with the presence of a pair of CNWs, where the corresponding cross sections at which the potential distributions were exhibited are indicated by dashed lines, and the results are shown in (c, d), respectively. Owing to the large magnitude variation in the potential distribution across the cross section, we use both color grade and equal potential lines to present the local potential. The blank region close to the CNWs is the region where the calculated piezopotential is smaller than -0.4 V, beyond the range selected for the color plotting. In order to show the detail in this region, we only used equal potential lines to present it. The CNWs were positioned close to the bottom of the unit cell in (b) to ensure that they were under compressive strain once a transverse force was applied in order to match the experimental case. (e) We also calculated the potential induced by perfect cylindrical NWs (e.g., zero conical angle). The result indicated that there was no potential difference being generated at the two electrodes. Presented is the cross section output of the calculated piezopotential similar to part d. (f) Calculated potential difference between the top and bottom electrodes of a nanogenerator as a function of the thickness projected conical nanowire density. The distance between the top and bottom electrode was kept constant ($5 \mu\text{m}$). The density required for a uniform, fully packed, monolayer coverage of the substrate is $\sim 90000/\text{mm}^2$.

presented remains valid. Once the applied stress is withdrawn, the strain in the CNWs is released and so is the piezoelectric field; the inductive charges in the electrode plates have to flow back. This is the process of producing an ac output current.²²

For easy visualization of the calculated potential, the orientation relationship between the realistic model for the measurement (Figure 2a) and the representing cross sections (Figure 2b) at which the distribution of the potential were exhibited (Figure 2c and 2d) can be correlated by the (x, y, z) coordinate as indicated in the corresponding figures. The piezopotential inside the CNWs is rather high so that it is plotted separately in Figure 2c. Owing to the conical shape of the nanowires and the opposite c axis, the piezopotentials inside the two CNWs are opposite in sign under compressive strain, but with a small separation in the charge centers in the direction normal to the substrate surface, which is the

fundamental mechanism for creating the inductive charges at the top and bottom electrodes. By adjusting the display scale of the piezopotential in the space outside of the CNWs, a 0.8 V inductive potential difference across the two electrodes is clearly shown (Figure 2d), which is generated by an applied compressive strain of 0.12% at the fixed end of the CNW (maximum strain). This is the driving force for the ac nanogenerator. As a verification of the conical shape of the NW being the key of the piezopotential in our design, a calculation for cylindrical nanowires²³ with zero conical angle showed that there is no potential difference across the two electrodes (Figure 2e). Our calculation also predicts that the voltage across the top and bottom electrodes is approximately proportional to the thickness projected density of CNWs if the total deposition is less than a monolayer (Figure 2f).

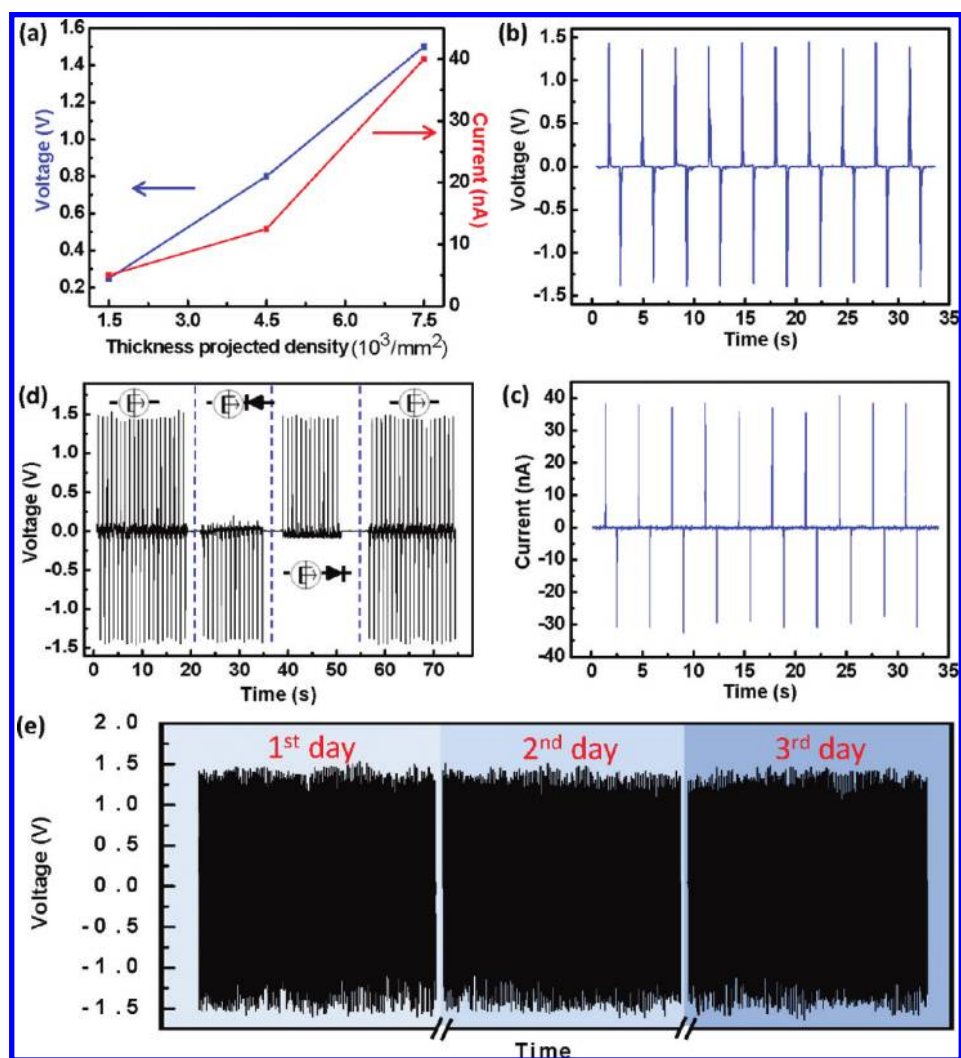


FIGURE 3. The performance of a packaged nanogenerator. (a) The measured output of a NG as a function of the thickness projected CNWs density. (b) The measured output voltage and (c) output current of a nanogenerator made of CNWs with a thickness projected density of 7000–7500/ mm^2 . (d) Output voltage of the nanogenerator before and after applying a diode to rectify the generated current. (e) The nanogenerator was tested for 3 days to examine its stability. The nanogenerator was continuously run each day for 3 h at a frequency of 1.64 Hz.

We first tested the nanogenerator with only one cycle of ZnO CNW deposition, corresponding to an area density of 1400–1500 CNWs/ mm^2 . Note the deposition density of the CNWs was rather low in comparison to a uniform and fully packed monolayer of CNWs of density $\sim 90000/\text{mm}^2$. The measured output voltage was ~ 0.25 V, and the output current was ~ 5 nA (Figure S7a,b in the Supporting Information) when strained to 0.11% at a straining rate of $3.67\% \text{ s}^{-1}$.²⁴ The output of the NG is approximately linearly proportional to the thickness-projected density of the CNWs (Figure 3a), in agreement with the theoretical prediction (Figure 2f). After the cycles of deposition of CNWs were increased to 5, corresponding to a thickness projected density of 7000–7500 CNWs/ mm^2 , the output voltage was raised to 1.5 V and the current to 30–40 nA (Figure 3b,c). The output current can be rectified using a diode (Figure 3d)

and stored for later use. The device showed good stability after 3 days of testing (Figure 3e).

We have carried out a series of controlled experiments to verify the working mechanism proposed in Figure 2. The first experiment was to replace the CNWs with cylindrical NWs with uniform cross section. After testing more than 10 such devices, the output voltage was typically < 10 mV and the output current was < 20 pA, which are 50 times and 200 times smaller than those received for the NG made of CNWs (Figure S7 in the Supporting Information). The second experiment was to fabricate a device as shown in Figure 1 but without depositing any NWs. The output was in the same order as that in the previous case (Figure S7 in the Supporting Information). In those measurements, one must be cautious to rule out possible artifacts from the measurement system and the capacitance of the device. In general, an

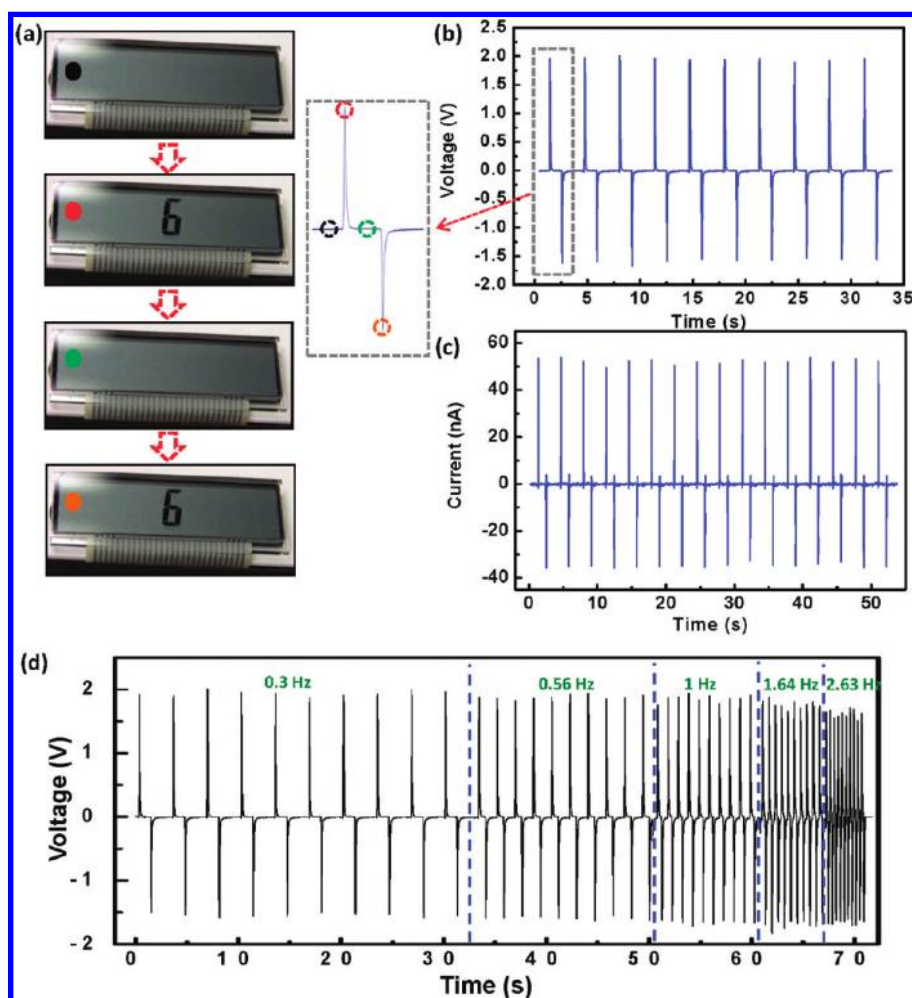


FIGURE 4. Driving a commercial LCD by a nanogenerator. (a) Four snapshots taken from a full cycle driving of a LCD by the NG at a frequency of 0.3 Hz. (b) and (c) Measured output voltage and output current of the NG. The right-hand part of (a) is an enlarged single cycle of the NG output. We use the dotted circle marked in different colors to show the LCD blinking in corresponding to each ac output peak of the NG. The LCD was taken from a calculator; only a small segment of the entire display area was powered by the NG. (d) The output of the NG with the increase in driving frequency, showing its good stability.

electrical measurement system has a feed in bias current in an order of picoamperes that may charge up the capacitor made of the two electrodes on the top and bottom surfaces; a variation in capacitance as a result of bending the entire structure may induce a small output voltage in the order of a few millivolts, but no output is as large as the ones shown in Figure 3. Finally, instead of using a solution to dispose the CNWs and then deposit them onto the substrate, we transferred the CNWs directly onto the substrate by dry physical contact, so that the CNWs were crossed and had a poor alignment with the substrate. In such a case, the fabricated NG gave an output voltage of 20–60 mV. These experiments show that the utilization of conical NWs is likely the key for receiving a large output voltage on the order of 1 V. The mechanism of the NG was proposed after studying more than 50 working devices (out of 100 totally fabricated) using the CNWs following the design shown in Figure 1.

The output power of the NG is sufficient to drive a LCD screen. An LCD is a nonpolar device that can be driven

directly by ac power as long as its output potential exceeds a threshold value. The LCD screen used for the test was taken from a Sharp calculator; a proper connection combination was chosen to get an output of number “6” at the front panel; the lighting area had a size about the same as that of the NG. The LCD screen was directly connected to a NG without involvement of any external sources or measurement meters. Figure 4a shows a series of snapshots taken for a full cycle driving of a LCD by the NG at a frequency of 0.3 Hz, showing the LCD blinking corresponding to each ac output peak of the NG. The output was measured to be 2 V in voltage (equivalent to an open circuit voltage of 3.3 V) and 50 nA in current (Figures 4b,c). Thus, the LCD screen blinked when a periodical mechanical deformation of strain 0.11 % at a straining rate of 3.67 % s⁻¹ was applied to the NG. The output of the NG was not affected significantly by an increase in the driving frequency (Figure 4d), and the power output at each peak was able to drive the LCD (see video 1 in the Supporting Information).

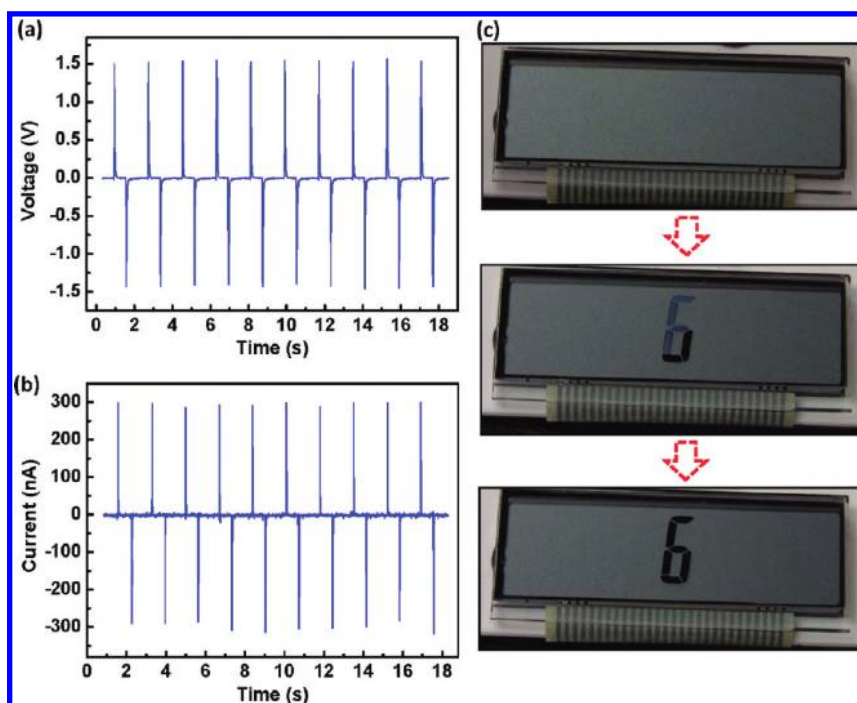


FIGURE 5. Continuous driving of a commercial LCD by a nanogenerator at a mechanical straining frequency of 0.56 Hz. (a, b) The measured output voltage and current of the NG, with peak voltage of 1.5 V and current of 300 nA. (c) Three snapshots taken from the LCD when the NG was periodically strained at a frequency of 0.56 Hz, showing that part of the character “6” was lit up and then all of the segments were continuously lit afterward.

The construction of the LCD screen can be regarded as some liquid crystal insert between two electrode plates. Thus this load is equivalent to a capacitor, C_{LCD} , with a parallel connected leakage resistance, R_{LCD} , as shown in the equivalent circuit in Figure S8 (in the Supporting Information). Considering the resistance of our voltage and current measurement equipments,²⁴ using the measured voltage and current values, the equivalent inner resistance R_{G} of this NG was derived to be 66.7 M Ω , and the maximum output power could reach ~ 42 nW.

The NG can continuously light a LCD. An LCD screen is a capacitive device that can release the input charges within a period of time, during which it continuously lights up if the electric field generated by the remaining stored charges is above the threshold. This is possible if the LCD discharging time is longer than the time interval between two consecutive mechanical straining actions, and its charging time is shorter than the response time of the human eye. Parts a and b of Figure 5 show the performance of an NG with an output voltage of 1.5 V and current of 300 nA. The equivalent inner resistance of this NG was ~ 5.3 M Ω , and the maximum output power was calculated to be ~ 118 nW. When the LCD screen was powered by the NG, it showed a continuous lighting up status (Figure 5c) (see video 2 in the Supporting Information). From the video we can see that the screen was blinking at first, then part of the segments were lit continuously. Finally, after several cycles, it reached an equilibrium lighting status for the full character. This means that our

nanogenerator can produce enough power to continuously drive an LCD.

There are several advantages for using nanowires rather than thin films for energy harvesting. First, the growth of a single crystal ZnO thin film needs to be done at a high temperature (typically >400 °C),^{25–27} which limits the choice of substrates especially for flexible electronics. With nanowires, although they need to be grown at relatively high temperature, transferring the nanowires from the growth substrate to any other substrate is an easy and simple process using our “dropping-on” technique (see Figure 1a). Second, the composited structure of ZnO and PMMA is much more flexible than ZnO thin films. In order to test the flexibility of a ZnO thin film, we sputtered a 100 nm thick ZnO film on a Kapton substrate that was covered with PMMA. Figure S9 (in the Supporting Information) shows scanning electron microscopy images of ZnO film before and after being stressed to 0.1 % compressive strain. We can see that there are lots of crack lines in the film perpendicular to the bending direction. While for the composite structure of ZnO nanowires and PMMA, there was no crack after being strained to the same degree for several days.

In comparison to our previously demonstrated approaches,^{15,16} our new method has the following unique advantages. First, the CNWs are fully enclosed by polymer without direct contacting with the electrodes. This noncontact design is likely to offer a robust nanogenerator with high stability. Second, from the fabrication process presented in

Figure 1 and Figure S1 in the Supporting Information, the fabrication procedures for the NG are simple and cost-effective. Finally, the approach has the potential for scale up, and it is likely to be adaptable for industrial mass production.

In summary, utilizing the conical shape of the ZnO nanowires, a nanogenerator is fabricated by simply dispersing them onto a flat PMMA film to form a rational “composite” structure. The flat PMMA surface may lead to a projected c axis unipolar assembly of the conical nanowires in the direction perpendicular to the substrate, which produces a macroscopic piezoelectric potential across the thickness of the structure by mechanical deformation. It is suggested that the observed ac current is from the dynamic flow of inductive charges between the top and bottom surface electrodes of the structure subjected to dynamic mechanical straining. For a nanogenerator with a thickness projected nanowire density of 7000/mm² and physical size of 1.5 × 2 cm², compressive strain of 0.11 % at a straining rate of 3.67 % s⁻¹ produces an output voltage up to 2 V (equivalent open circuit voltage of 3.3 V), which has been shown to drive a commercial liquid crystal display (LCD). Importantly, the size of the NG used for driving the LCD had a size that was comparable to the size of the lighting area, so that it could be integrated at the back of the LCD, indicating its possibility for live-driving of a flexible display. Our nanogenerator is a simple, cost-effective, and scalable technology for small personal electronics and self-powered systems.

Acknowledgment. Research was supported by DARPA (HR0011-09-C-0142, Program manager, Dr. Daniel Watten-dorf), Airforce, BES DOE (DE-FG02-07ER46394), and NSF (CMMI 0403671).

Supporting Information Available. Additional figures showing structure of the nanogenerator, conical shape of the grown nanowires, random dispersion of the conical nanowires, and assembly of the nanowires on a flat substrate calculation of the potential drop across the composite structure, and videos showing lighting of an LCD powered by a nanogenerator and continuous lighting of an LCD by a nanogenerator. This material is available free of charge via the Internet at <http://pubs.acs.org>.

REFERENCES AND NOTES

- (1) Oregan, B.; Gratzel, M. *Nature* **1991**, *353*, 737.
- (2) Huynh, W. U.; Dittmer, J. J.; Alivisatos, A. P. *Science* **2002**, *295*, 2425.

- (3) Baxter, J. B.; Aydil, E. S. *Appl. Phys. Lett.* **2005**, *86*, No. 053114.
- (4) Law, M.; Greene, L. E.; Johnson, J. C.; Saykally, R.; Yang, P. *Nat. Mater.* **2005**, *4*, 455.
- (5) Tian, B.; Zheng, X.; Kempa, T. J.; Fang, Y.; Yu, N.; Yu, G.; Huang, J.; Lieber, C. M. *Nature* **2007**, *449*, 885.
- (6) Fan, Z.; Razavi, H.; Do, J.; Moriwaki, A.; Ergen, O.; Chueh, Y.-L.; Leu, P. W.; Ho, J. C.; Takahashi, T.; Reichertz, L. A.; Neale, S.; Yu, K.; Wu, M.; Ager, J. W.; Javey, A. *Nat. Mater.* **2009**, *8*, 648.
- (7) Weintraub, B.; Wei, Y.; Wang, Z. L. *Angew. Chem., Int. Ed.* **2009**, *48*, 1.
- (8) Wang, Z. L.; Song, J. *Science* **2006**, *312*, 242.
- (9) Wang, X.; Song, J.; Liu, J.; Wang, Z. L. *Science* **2007**, *316*, 102.
- (10) Qin, Y.; Wang, X.; Wang, Z. L. *Nature* **2008**, *451*, 809.
- (11) Chang, C.; Tran, V. H.; Wang, J.; Fuh, Y.-K.; Lin, L. *Nano Lett.* **2010**, *10*, 726.
- (12) Choi, D.; Choi, M.-Y.; Choi, W. M.; Shin, H.-J.; Park, H.-K.; Seo, J.-S.; Park, J.; Chae, S. J.; Lee, Y. H.; Kim, S.-W.; Choi, J.-Y.; Lee, S. Y.; Kim, J. M. *Adv. Mater.* **2010**, *22*, 2187.
- (13) Xu, S.; Qin, Y.; Xu, C.; Wei, Y.; Yang, R.; Wang, Z. L. *Nat. Nanotechnol.* **2010**, *5*, 367.
- (14) Yi, Q.; Jafferis, N. T.; Lyons, K.; Lee, C. M.; Ahmad, H.; McAlpine, M. C. *Nano Lett.* **2010**, *10*, 524.
- (15) Chen, X.; Xu, S.; Yao, N.; Shi, Y. *Nano Lett.* **2010**, *10*, 2133.
- (16) Zhu, G.; Yang, R.; Wang, S.; Wang, Z. L. *Nano Lett.* **2010**, *10*, 3151.
- (17) Yu, C. H.; Shi, L.; Yao, Z.; Li, D.; Majumdar, A. *Nano Lett.* **2005**, *5*, 1842.
- (18) Dresselhaus, M. S.; Chen, G.; Tang, M. Y.; Yang, R. G.; Lee, H.; Wang, D. Z.; Ren, Z. F.; Fleurial, J.-P.; Gogna, P. *Adv. Mater.* **2007**, *19*, 1043.
- (19) Poudel, B.; Hao, Q.; Ma, Y.; Lan, Y.; Minnich, A.; Yu, B.; Yan, X.; Wang, D.; Muto, A.; Vashaee, D.; Chen, X.; Liu, J.; Dresselhaus, M. S.; Chen, G.; Ren, Z. *Science* **2008**, *320*, 634.
- (20) Song, J.; Wang, X.; Riedo, E.; Wang, Z. L. *J. Phys. Chem. B* **2005**, *109*, 9869.
- (21) Gao, Y. F.; Wang, Z. L. *Nano Lett.* **2007**, *7*, 2499.
- (22) Yang, R. S.; Qin, Y.; Dai, L. M.; Wang, Z. L. *Nat. Nanotechnol.* **2009**, *4*, 34.
- (23) The true cross section of a ZnO nanowire is hexagonal. For easy description in this paper, we approximately take a hexagonal nanowire as a cylindrical nanowire for easy computation. By the same token, the conical nanowire means hexagonal conical nanowires. Such an approximation does not affect the conclusion.
- (24) The relationship between the measured output voltage V and the open circuit voltage V_{oc} of the NG is $V = V_{oc}R_m/(R_G + R_m)$, where R_G is the inner resistance of the NG and $R_m = 100 \text{ M}\Omega$ is the resistance of the voltmeter. This means that the true open circuit voltage can be significantly larger than the measured output voltage if R_G is comparable to R_m . The measured output current I is related to the short circuit current I_{sc} by $I = I_{sc}R_G/(R_G + R_m')$, where R_m' is the resistance of the amperemeter, which is 100Ω with a sensitivity of 10^{-6} A/V and $10 \text{ k}\Omega$ with a sensitivity of 10^{-7} A/V .
- (25) Chen, Y.; Bagnalla, D. M.; Zhua, Z.; Sekiuchia, T.; Parka, K.-T.; Hiragaa, K.; Yao, T.; Koyamab, S.; Shenb, M. Y.; Gotob, T. *J. Cryst. Growth* **1997**, *181*, 165.
- (26) Gorla, C. R.; Emanetoglu, N. W.; Liang, S.; Mayo, W. E.; Lu, Y.; Wraback, M.; Shen, H. *J. Appl. Phys.* **1999**, *85*, 2595.
- (27) Muth, J. F.; Kolbas, R. M.; Sharma, A. K.; Oktyabrsky, S.; Narayan, J. *J. Appl. Phys.* **1999**, *85*, 7884.